International Journal of Innovative Technology and Exploring Engineering (IJITEE)
ISSN: 2278-3075 (Online), Volume-6 Issue-3, August 2016

Theoretical Study of Vertical Parallel Junction Silicon Solar Cell Capacitance under Modulated Polychromatic Illumination: Influence of Irradiation

Ndèye Madeleine DIOP, Boureima SEIBOU, Mamadou WADE, Marcel Sitor DIOUF, Ibrahima LY, Hawa LY DIALLO, Grégoire SISSOKO

***Abstract:** This article is a theoretical study of vertical parallel junction silicon solar cell capacitance under modulated polychromatic illumination: influence of irradiation. Thus, from the minority carrier density and the photovoltage expressions, the capacitance is determined. Furthermore, Bode and Nyquist diagram followed by an equivalent electric circuit of the capacitance is given.*

***Keywords:** solar cell vertical junction - frequency–Capacitance-irradiation – photovoltage - Nyquist-Bode.*

I. INTRODUCTION

Solar energy is an inexhaustible energy source. Solar cell technology has been pioneered in space industry, essentially because solar energy is one of the main power sources for satellites. However, space environment is a very harsh environment for electronic devices, such as silicon solar cells and other semiconductor based detectors. We can obtain energy by converting the solar energy in electrical energy with the semiconductor optoelectronic device such as the vertical junction solar cell [1] or horizontal junction [2-3]. The quality of a solar cell is related to its electronic [4] and electrical [5] parameters. The aim of this study is to show the influence of the irradiation energy under frequency modulation on a silicon solar cell, especially for the following parameters: Relative excess minority carrier density, photovoltage, and capacitance.

II. THEORY

A solar cell is an electronic component that converts sunlight into electricity. This conversion is performed by using a photovoltaic cell in parallel vertical junction. Figure1 represents an n-p-n type of a parallel vertical junction of a photovoltaic cell.

Manuscript published on 30 August 2016.
*Correspondence Author(s)
Ndèye Madeleine DIOP, Faculty of Science and Technology, Cheikh Anta Diop University, Dakar, Senegal.
Boureima SEIBOU, Ecole Des Mines DE L'Industrie ET De La Geologie, Niamey – Niger.
Mamadou WADE, Ecole Polytechnique de Thiès, University in the Roman Catholic Diocese of Thiès, Senegal.
Marcel Sitor DIOUF, Faculty of Science and Technology, Cheikh Anta Diop University, Dakar, Senegal.
Ibrahima LY, Ecole Polytechnique de Thiès, University in the Roman Catholic Diocese of Thiès, Senegal.
Hawa LY DIALLO, Faculty of Science and Technology, Université de Thiès, Thies, Senegal.
Grégoire SISSOKO, Faculty of Science and Technology, Cheikh Anta Diop University, Dakar, Senegal.

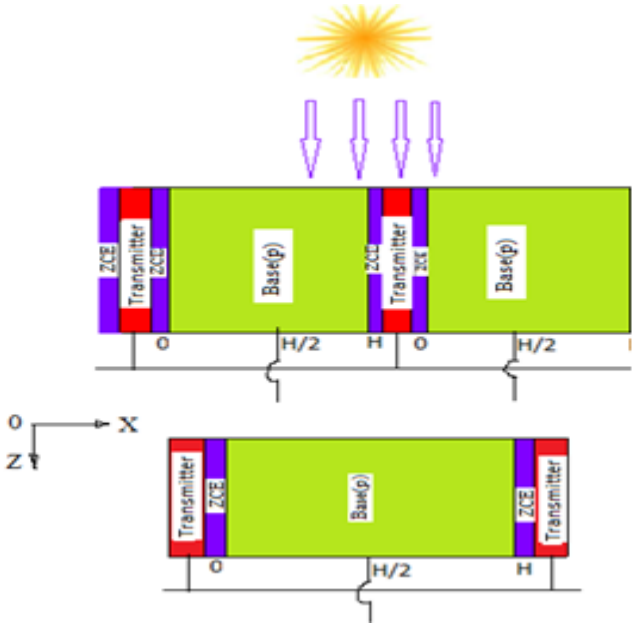

Figure1: Schematic structure of a vertical junction solar cell

2.1. Study Of The Relative Minority Carrier Density Inthe Base Continuity Equation

The continuity equation governing the phenomena which take place in the base is giving by the following expression:

$$D(\omega, kl, \phi_p)\frac{\partial^2 \delta(x,t)}{\delta x^2} - \frac{\partial(x,t)}{\tau} = -G(z,t) + \frac{\partial \delta(x,t)}{\partial t} \quad (1)$$

G (z) is the global carrier generation rate at depth z in the base[6] [7]

$$G(z) = \sum_{i=1}^{3} a_i e^{(-biz)} e^{(j\omega t)} \quad (2)$$

a_i and b_i are tabulated coefficients of the radiation deduced from the generation rate modeling considered for overall the solar radiation spectrum when AM=1.5 **[8]**

ω is the angular frequency

$$\delta(x,t) = \delta(x)e^{(j\omega t)} \quad (3)$$

Published By:
Blue Eyes Intelligence Engineering and Sciences Publication (BEIESP)

Table 1: Various (different) values of the tabulated coefficients ai and bi under AM =1.5

a_i ($cm^{-3}.s^{-1}$)	b_i (cm^{-1})
a_1=6,13.10^{20}	b_1=6630
a_2=0,54.10^{20}	b_2=1000
a_3=0,0991.10^{20}	b_3=130

$D(\omega,\phi_p,kl)$ is the diffusion coefficient in dynamic frequency mode (regime) under irradiation

$D(\omega,\phi_p,kl)$ is given by the following relation[9].

$$D(\omega,kl,\phi_p)=D(kl,\phi_p)\left[\frac{1+\omega^2\tau^2}{(1-\omega^2\tau^2)+(2\omega\tau)}+\frac{-\omega^2\tau^2-1}{(1-\omega^2\tau^2)^2+(2\omega\tau)^2}j\right] \quad (4)$$

$$D(kl,\phi_p)=\frac{L(kl,\phi_p)^2}{\tau} \quad (5)$$

$L=\sqrt{\tau D}$ is the diffusion length

Using the boundary conditions, the solution for equation (1) is given as follow.

$$D(\omega,kl,\phi_p)\frac{\partial^2\delta(x)}{\delta x^2}e^{(j\omega t)}-\frac{\partial(x)e^{(j\omega t)}}{\tau}= -\sum_{n=1}^{3}a_i e^{(-biz)}e^{(j\omega t)}+\frac{\partial\delta(x)e^{(j\omega t)}}{\partial t} \quad (6)$$

a) at the junction x = 0

$$\left[D(\omega,kl,\phi_t)\frac{\partial\delta(x)}{\partial x}\right]_{x=0}=[Sf\delta(x)]_{x=0} \quad (7)$$

Sfis recombination velocity at the junction [10, 11]

b) In the middle of the base $x=\frac{H}{2}$

$$\left[D(\omega,kl,\phi_t)\frac{\partial\delta(x)}{\delta x}\right]_{x=\frac{H}{2}}=0 \quad (8)$$

The general solution ofequation1is given by:

$$\delta(x)=\left[\frac{L(\omega,kl,\phi_t)^2}{D(\omega,kl,\phi)_t}\sum_{n=1}^{3}a_i e^{(-b_i z)}+A\cosh\left[\frac{x}{L(\omega,kl,\phi_t}\right]+B\left[\frac{x}{L(\omega,kl,\phi_t}\right]\right] \quad (9)$$

$\delta(x)$: is the minority carrier density

A and B to be determined by means of the boundary conditions.

In our next pages the relative minority carrier density of the solar cell versus the base depth for various parameters are investigated:

a) Damage coefficient effect in short circuit
b) Irradiation energy effect in short and open circuit
c) Frequency effect in short and open circuit

A. Effect of the damage coefficient in short circuit

The following graph is the relative minority carrier density of the solar cell Near the short circuit versus the depth of the base for various damage coefficient

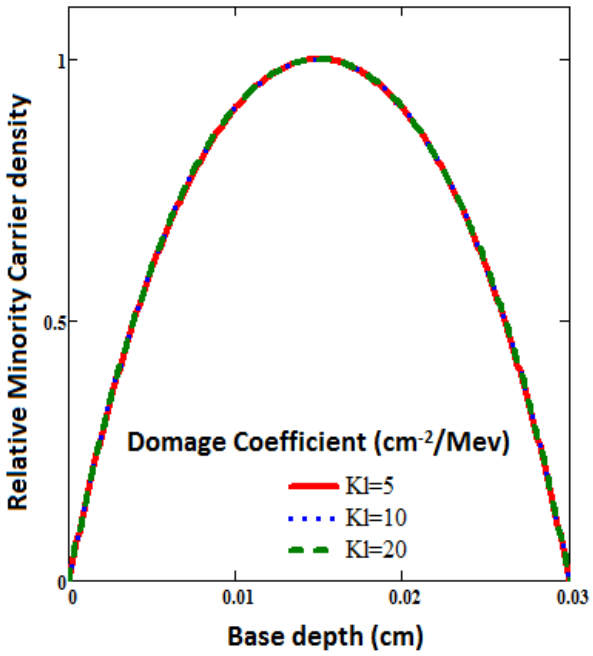

Figure 2:Relative minority carrier density versus base depth for various damage coefficients (z=0.001cm, ω=10^3rad/s, Sf=10^6cm/s,Φp=100MeV)

We observe:

A maximum at x=0.015cm, On both sides of it we note two types of gradients for a solar cell:

The relative minority carrier density increases from x=0 to x=0.015 (the increasing part of the curve) for the left emitter, and from x=0.015 to x=0.030cm (the decreasing part of the curve) for the right emitter. It also increases with the frequency too.

The gradient is thus positive for in the two localized zones x<0.015 and x>0.015. As the gradient is positive for the latter, the number of minority carriers crossing the junction is much greater, and those reaching the edge of the depletion zone contribute to the photocurrent.

At x=0.015, where the relative minority carrier density reaches its maximum, the gradient is null and the carriers are blocked. This value corresponds to the open circuit.

That the graph remains unchanged whatever damage coefficient values are.

We present on figure 3, 4the relative minority carriers density versus base depth for various irradiation energy.

Published By:
Blue Eyes Intelligence Engineering
and Sciences Publication (BEIESP)

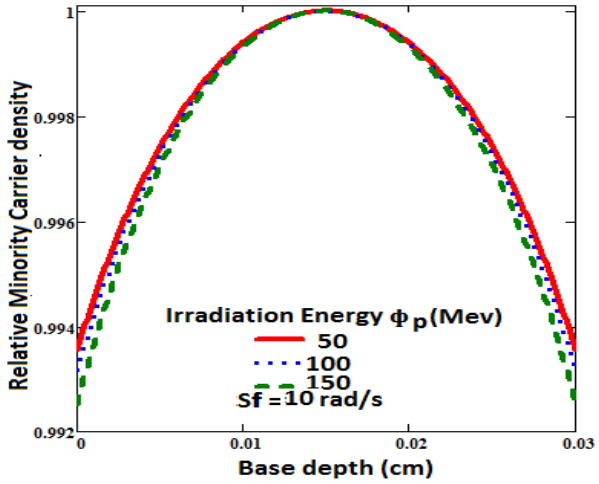

Figure 3: near the open circuit

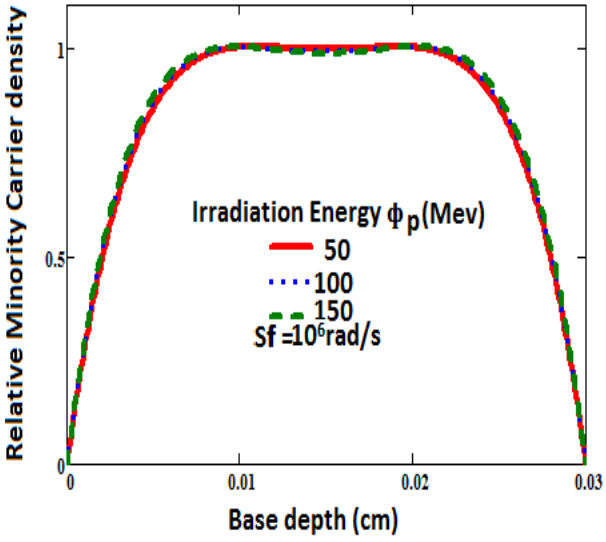

Figure 4: near the short circuit

Figure 3and 4: Relative minority carrier density versus base depth for various particle energy. (z=0.001cm, ω=10⁶rad/s, kl=15cm^{-2}/MeV)

The relative minority carrier density increases with increasing depth of the base up to the value x = x0 and also increases with the irradiation energy. in this region, the gradient is positive more carriers traverse the junction and participate to photocurrent.

At x=0.015, where the relative minority carrier density reaches its maximum, the gradient is null and the carriers are blocked. This value corresponds to the open circuit. Furthermore, we note that the two graphs reflect virtually the same trends of the carrier density, the fundamental difference lying in the behavior of the density when it reaches its maximum. Indeed, the solar cell density in open circuit situation has a bearing whereas short-circuit we notice a spike in x0.

The gradient is thus positive for in the two localized zones x<0.015 and x>0.015. As the gradient is positive for the latter, the number of minority carriers crossing the junction is much greater, and those reaching the edge of the depletion zone contribute to the photocurrent We present on figure 5 the relative minority carrier density versus base depth for various frequency.

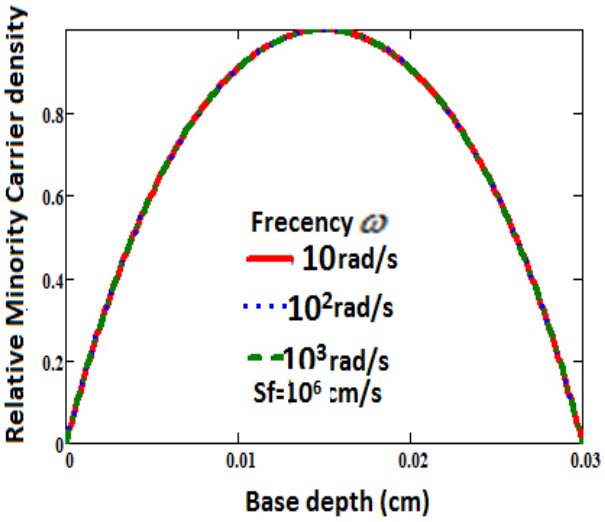

Figure 5 near the open circuit

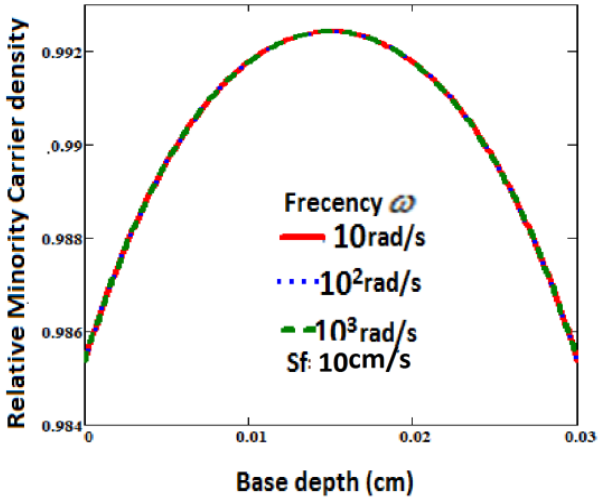

Figure 6 near the short circuit

Figure 5, 6: Relative minority carrier density versus base depth for various particle energy. (z=0.001cm, Φp=100MeV, kl=15cm^{-2}/MeV)

The relative minority carrier density increases with increasing depth of the base up to x0 and also increases with the frequency. The positive gradient in this zone mean more carriers traverse the junction and participate to photocurrent.

A zero gradient at the maximum density value: in this position the carriers are blocked at the junction; it is an open circuit situation. for low frequency values, we also notice that for the solar cell near open circuit the carriers are blocked at the junction for several values of the base depth, unlike the solar cell near short circuit, zero gradient is located just at the position x = x0. The positive gradient when x greater than x0 the relative density decreases with increase of the base depth all carriers in this zone traverse the junction and participate to photocurrent.

We present on figure 7, 8 the relative minority carrier density versus base depth for various frequency.

Published By:
Blue Eyes Intelligence Engineering and Sciences Publication (BEIESP)

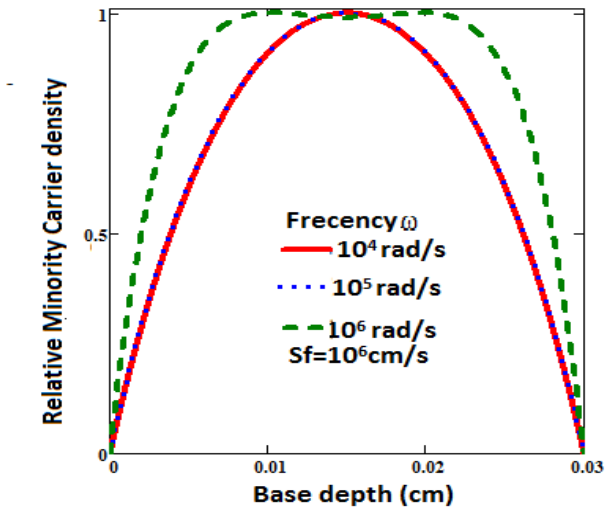

Figure 7 near the open circuit

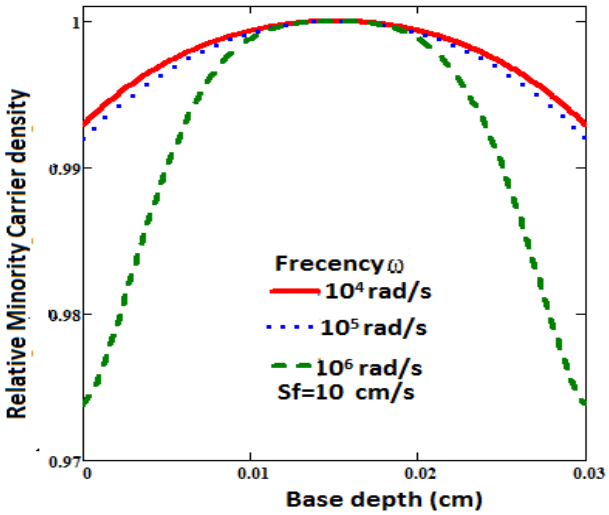

Figure 8 near the short circuit

Figure 7, 8: relative Minority carriers density versus base depth for various frequency (z=0.001cm, Φp=100MeV, kl=15cm^{-2}/MeV)

The relative minority carrier density increases with the base depth until a maximum value and then decreases gradually. We observe two types of gradients.

A positive gradient when x <x0 and x> x0 in these regions all the carriers cross the junction and are involved in photocurrent.

At position x = x0 the gradient is nil carriers are blocked at the junction. When the solar cell is in open circuit at 10^5 rad / s frequency ,fewer minority carriers participate to the photocurrent. But when the solar cell is near short circuit at 10 ^{5}rad / s frequency all carriers participate to the photocurrent.

Furthermore, we note that the two graphs reflect virtually the same trends of the carrier density, the fundamental difference lying in the behavior of the density when it reaches its maximum. Indeed, the solar cell density in open circuit situation has a bearing whereas short-circuit we notice a spike in x0.

2.2. Photo voltage

From Boltzmann law, the photovoltage can be written as:[12, 13,14]

$$V_{ph} = V_T . \ln\left(1 + \frac{N_b}{n_i^2} . \delta(x)\Big|_{x=0}\right)$$

$$V_T = \frac{K_b . T}{q} \qquad (11)$$

Where NB, VT, Kb and T are respectively the base doping density and the thermal voltage the Boltzmann constant andT the absolute temperature.

The figure below shows the photovoltage versus recombination velocity for various particle energy.

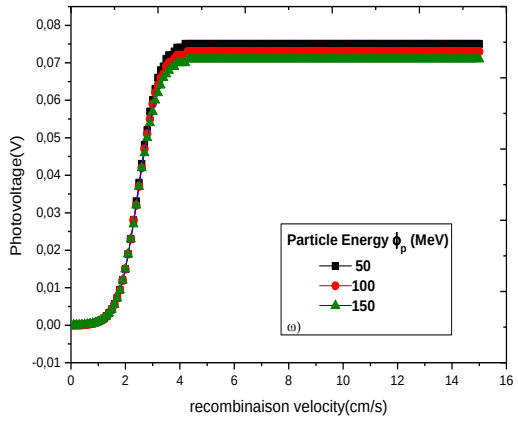

Graph10: Photovoltage versus recombination velocity for various types of particle energy (z=0.001cm, kl=15cm^{-2}/MeV,ω=10^5rad/s)

The photvoltage density increases with the decrease of the recombination velocity.

We have two areas: the first one corresponding to the open circuit where the photovoltage is at its maximum value and it's constant .Indeed, near open circuit the carriers are accumulated at the junction there by increasing the probability of interaction with the particles radiation an therefore the damage; the last one corresponding to the short-circuit situation where the photo voltage increases very rapidly towards a maximum value .Increasing irradiation energy decreases the photovoltage across the solar cell.

2.3. Capacitance

The diffusion capacitance of the solar cell is considered to be the capacitance resulting of a charge variation through diffusion process in the solar cell [13, 15, 16]. This capacitance can be written as:

$$C = q \cdot \frac{\partial \delta(x,z)}{\partial V_{ph}}\bigg|_{x=0} \qquad (13)$$

$$C = \frac{q \cdot n_o}{V_T} + q \cdot \frac{\delta(0,z)}{V_T} \qquad (14)$$

Published By:
Blue Eyes Intelligence Engineering
and Sciences Publication (BEIESP)

The diffusion capacitance consists of two terms; the first term is the intrinsic capacitance and the second depend on the operating point.

$n_o = \frac{n_i^2}{N_B}$ is the equilibrium concentration of minority carriers in the base We present in the figure below the capacitance versus recombination velocity for various damage coefficient.

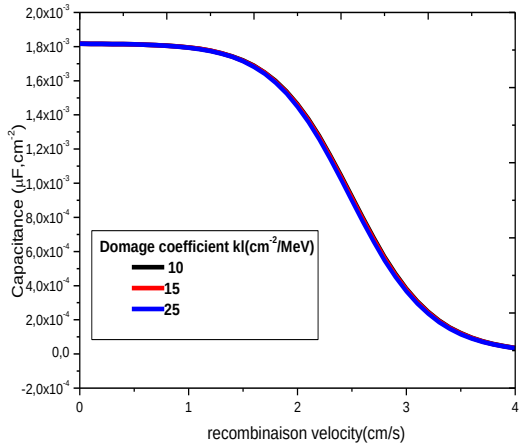

Figure 11: Capacitance versus Junction recombination velocity for various types of damage coefficient (Φp=100MeV, z=0.001cm, ω=10^{5}rad/s)

We note that the maximum capacitance then decreases sharply until practically a minimum value. When damage coefficient increases, we see a decreased capacitance of the solar cell and especially for low values of the recombination velocity so near the open circuit. This means that it is when we have a large accumulated charge that damage are most noticeable.

In the figure12 below the capacitance versus recombination velocity for various frequency is studied.

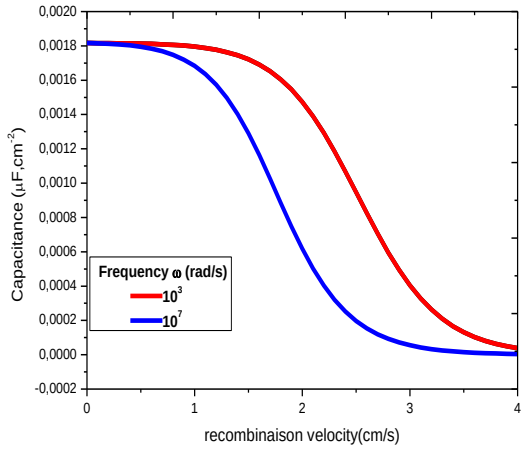

Figure 12: Capacitance versus Junction recombination velocity for various frequency (Φp=100MeV, z=0.001cm)

We find that the capacitance de creases with increasing recombination velocity. The solar cell capacitance is constant whatever the frequency value. In both situations: open and short circuit but for the intermediate values of the recombination velocity capacity decreases more quickly and reaches faster the short circuit situation. The open circuit capacitance is greater than the short circuit capacitance.

In the following the study we present the Nyquist diagram for different types of particle energy [17]: Irradiation energy effect in short and open circuit

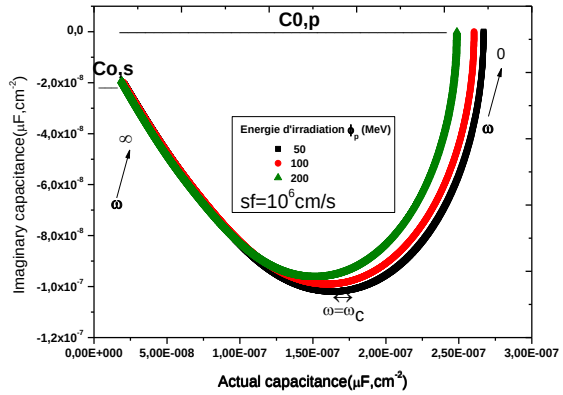

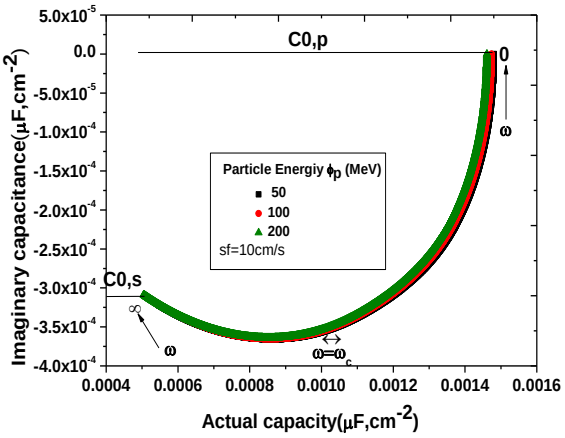

Figure 13:Imaginary capacitance versus Real Capacitance for various particle energyvalues. (z=0.001cm, kl=15cm^{-2}/MeV)

.The Nyquist diagram of a parallel R-C network is shown in *Figure 14, 15.*The capacitance spectrum is a semicircle, with its radius equal to 'R/2'. The semicircle is in the fourth quadrant, the real axis and does not touch the origin near short circuit. The open circuit capacitance is greater than the short circuit capacitance. This confirms that the radius near open circuit is greater than the radius short circuit. We present in the figure below the Bode diagram of the capacitance

Published By:
Blue Eyes Intelligence Engineering and Sciences Publication (BEIESP)

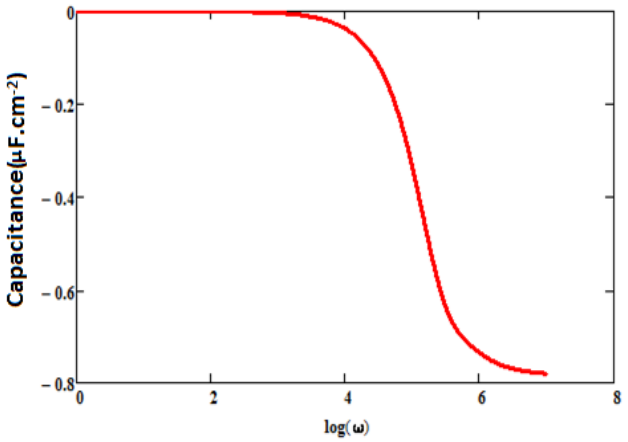

Figure16: Bode diagram of the capacitance (kl=10cm^{-2}/MeV, z=0,01cm,Sf=10^{3}cm/s,Φp=100MeV)

We now plot on Fig. 16 the capacitance of the cell versus modulation frequency in semi-logarithmic scale (Bode diagram).

This figure shows that the capacitance decreases with increasing modulation frequency.

We note that the code of static regime phase is maximum and constant then abruptly decreases in dynamic mode to negative values equivalent electrical models deduced from Bode and Nyquist diagram reflecting the resistive and capacitive effects.

We present in the scheme below equivalent electrical circuit of capacitance near short circuit

2.4. technical determination of the equivalent electric model of C0 [18]:

$$z = \frac{R_p + jX_p}{R_p + jX_p}$$

$$Z = \frac{jR_pX_p^2}{R_p^2 + X_p^2} + \frac{jR_p^2X_p}{R_p^2 + X_p^2}$$

$$Z = R + jX$$

$$(X-a)^2 + (Y-b)^2 = r^2$$

$$Z = Rs + \frac{Rsh}{1+(\omega RshC)^2} - \frac{i(\omega R^2shC)}{1+(\omega RshC)^2} = Zc + Z_R$$

$$Zc = Rs + Z_R + \frac{Rsh}{1+(\omega RshC)^2} - \frac{i(\omega R^2shC)}{1+(\omega RshC)}$$

Sf=10^{6}cm/s Short circuit			
ϕ_P (MeV)	R_p (Ω.cm^2)	R_S (Ω.cm^2)	C (F)
50	3.35×10^{4}	2.9	2.46×10^{-7}
100	3.95×10^{4}	3.2	2.19×10^{-7}
200	4.08×10^{4}	3.38	2.07×10^{-7}

$$Zc = C0,s + Z_R + \frac{C0,p}{1+(\omega \times C0,p \times C)} - \frac{i(\omega \times C^2 0,p \times C)}{1+(\omega \times C0,p \times C)}$$

For this, we consider the center of a semicircle Δ((C0,s+C0,p /2);0) and radius R(C0,p /2).

Zc can be rewritten as the two components (real and imaginary part)

$$Zc = \mathrm{Re}(Zc) + j\,\mathrm{Im}(Zc) \qquad (18)$$

$$Zc = X + jY$$

With X= Re (Zc); Y=Im (Zc) and j the complex variable (j=√-1)

To simplify notations, we define the variables a and b; with a = C0,s and b = C0,p

Terms of the Zc are connected by the equation:

$$\left[X - (a + \frac{b}{2})\right]^2 + Y^2 = (\frac{b}{2})^2 \qquad (20)$$

The resolution of the equation leads to the determination of X and Y:

$$\begin{cases} X = \mathrm{Re}(Zc) = Co,s + Z_R + \dfrac{\omega \cdot C \cdot (C0,p)^2}{1+(\omega \cdot C \cdot C0,p)^2} & (21) \\ Y = \mathrm{Im}(Zc) = \dfrac{\omega \cdot C \cdot (C0,p)^2}{1+(\omega \cdot C \cdot C0,p)^2} & (22) \end{cases}$$

The characteristics of particular points are summarized by the following equations:

$\omega \to 0$

$$\begin{cases} X = \mathrm{Re}(Zc) = C0,s + C0,p & (23) \\ Y = \mathrm{Im}(Zc) = C0,p & (24) \end{cases}$$

$\omega = \omega_c$

$$\begin{cases} X = \mathrm{Re}(Zc) = C0,s + \dfrac{C0,p}{2} & (25) \\ Y = \mathrm{Im}(Zc) = \dfrac{C0,p}{2} & (26) \end{cases}$$

$\omega \to \infty$

$$\begin{cases} X = \mathrm{Re}(Zc) = C0,s & (27) \\ Y = \mathrm{Im}(Zc) = 0 & (28) \end{cases}$$

From the expressions obtained at ω→0 and ω = ω$_c$, we give the following table:

Sf=10^{2}cm/s Open circuit			
ϕ_P (MeV)	R_p(Ω.cm^2)	R_S(Ω.cm^2)	C (F)
50	47.015	1.54	9.8×10^{-4}
100	52.282	1.69	9.4×10^{-4}
200	55.87	1.89	9.2×10^{-4}

Knowing the values of the parallel resistor *Rp* and cut-off frequency value [3] we can deduce the capacity from the relationship:[19]

$$R_pC = \frac{2\pi}{\omega_c}$$

Published By:
Blue Eyes Intelligence Engineering and Sciences Publication (BEIESP)

From this **Table**, we find that when the value of the irradiation energy increases, the resistance decreases R_p which is due to the slowdown in minority carrier diffusion caused by irradiation. Consequently, the intrinsic properties of the solar cell are damaged; this implies a lower quality of the cells [20], [21].

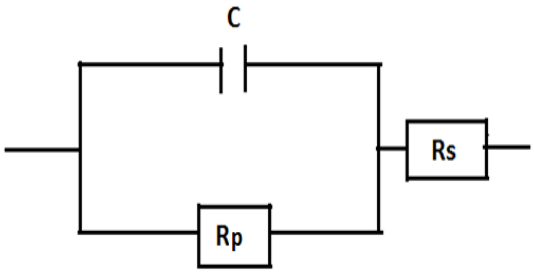

Figure 14: equivalent electrical circuit of capacitance near short circuit

III. CONCLUSION

The resolution of the continuity equation helped to determine the expression of the minority carrier density. This theoretical study highlighted the irradiation effect on the minority carrier density, on the photovoltage and on the capacitance of a parallel vertical junction silicon solar cell.

REFERENCES

1. M. L. Samb, M. Zoungrana, F. Toure, M. T. D. Diop, G. Sissoko. "Study in 3D modeling of a solar cell silicon static regime placed in a magnetic field and under constant multispectral illumination: Determination of electrical parameters" Journal des sciences Vol 10, N°4, 2010, pp. 23-38. www.cadjds.org
2. O. Sow, I. Zerbo, S. Mbodji, M.I. Ngom, M.S. Diouf and G. Sissoko, "Silicon solar cell under electromagnetic waves in steady state: electrical parameters determination using the i-v and p-v characteristics." International Journal of Science, Environment and Technology, 1(4), (2012). pp. 230 – 246.
3. Dieng, M.L. Sow, S. Mbodji, M.L. Samb, M. Ndiaye, M. Thiame, F.I. Barro and G. Sissoko, "3D study of polycrystalline silicon solar cell: influence of applied magnetic field on the electrical parameters." Semiconductor Science and technology, 26(9), (2011). pp. 473-476.
4. Mazhari and H.Morkoç, "Theoretical study of a parallel vertical multi-junction silicon", J. App. Phys. 73(11), (1993), pp. 7509-7514
5. H. EL .Ghitani and S. Martinuzzi, "Determination Electric parameters of a solar cell silicon" J. App. Phys. 66(4), (1989), pp. 1717-1726 .
6. J. Dugas, "3D Modelling of a Reverse Cell Made with Improved Multicrystalline Silicon Wafers", Solar Energy Materials and Solar Cells, 32, (1),(1994) pp. 71 – 88,.
7. K. Misiakos, C.H. Wang, A. Neugroschel, and F.A. Lindholm. "Simultaneous Extraction of minority-carrier parameters in crystalline semiconductors by lateral photocurrent". J. Appl. Phys. 67 (1), (1990). pp 321 – 333.
8. Sissoko, G., C. Museruka, A. Corréa, I. Gaye and A.L. Ndiaye,. "Light spectral effect on recombination parameters of silicon solar cell". Renew. Energ., 3, (1996), pp. 1487-1490.
9. Tall, B. Seibou, M. A. O. El Moujtaba, A. Diao, M. Wade, G. Sisoko, **"**Diffusion Coefficient Modeling of a Silicon Solar Cell under Irradiation Effect in Frequency: Electric Equivalent Circuit", International Journal of Engineering Trends and Technology (IJETT), 19, (2), (2015), pp. 56-61
10. Ricaud, Photopiles Solaires, Presses Polytechniques et Universitaires Romandes, 1997
11. M. L. Samb, M. Dieng, S. Mbodji, N. Thaim, F. I. Barro, G. Cisssoko "Recombination parameters measurement of silicon solar cell under constant white bias light". Proceedings of the 24th European Photovoltaic Solar Energy Conference, Germany (Hamburg), September (2009), pp.469-472
12. Sissoko, G., E. Nanéma, A. Corréa, P.M. Biteye, M. Adj and A.L. Ndiaye,. "Silicon Solar cell recombination parameters determination using the illuminated I-V characteristic. Renew. Energ., 3, (1998), pp. 1848-1851
13. H. L. Diallo, A. S. Maiga, A. Wereme, G. Sissoko "New approach of both junction and back surface recombination velocity in a 3D modelling study of a polycrystalline silicon solar cell. Eur. Phys. J. Appl. Phys. 42, (2008), pp. 203–211
14. Dione, M.M., S. Mbodji, M.L. Samb, M. Dieng, M.Thiame, S. Ndoye, F.I. Barro and G.Sissoko,. "Vertical Junction under Constant Multispectral Light: Determination of Recombination Parameters." Proceedings of the 24th European Photovoltaic Solar Energy Conference , Germany (Hamburg), September 2009, pp. 465- 468
15. Mbodji, S., B. Mbow, F. I. Barro, G.Sissoko, "a 3D model for thickness and diffusion capacitance of emitter-base junction determination in a bifacial polycrystalline solar cell under real operating condition." Turkish Journal of Physics, 35(3) , (2011), pp. 281 – 291.
16. Mbodji, S., M. Dieng, B. Mbow, F.I. Barro and G. Sissoko, ".Three dimensional simulated modelling of diffusion capacitance of polycrystalline bifacial silicon solar cell." Journal of Applied Science and Technology (JAST), 15(1 & 2), (2010), pp. 109 – 114
17. Mbodji, S., I. Ly, H.L. Diallo, M.M. Dione, O. Diasse and G. Sissoko, "Modeling study of n+/p solar cell resistances from single I-V characteristic curveconsidering the junction recombination velocity (Sf)", .Res. J. Appl. Sci. Eng. Techn., 4(1), (2012), pp. 1-7.
18. Anil Kumar, R "Measurement of solar cell AC parameter susing Impedance Spectroscop", A Thesis Submitted for the Degree of master of science (Engg,) in the Faculty of Engineerin Indian Institute of Science, Jan. 2000 pp. 49-50
19. El. Ndiaye, G. Sahin, M. Dieng, A. Thiam, H. L. Diallo, M. Ndiaye, G. Sissoko. "Study of the Intrinsic Recombination Velocity at the Junction of Silicon Solar under Frequency Modulation and Irradiation".J. Appl Math and Physics, 3, (2015), pp. 54-55
20. Mora-Sero, I., Garcia-Belmonte, G., Boix P.P., Vazquez, M.A. and Bisquert, J., "Impedance Spectroscopy Characterization of Highly Efficient Silicon Solar Cells under Different Illumination Intensities Light" .Energyand Environmental Science, 2, (2009), pp.678-686.
21. Suresh, S., "Measurement of Solar Cell Parameters Using Impedance Spectroscopy." Solar Energy Materials and Solar Cells, 43, (1996) , pp 21-28.

Published By:
Blue Eyes Intelligence Engineering and Sciences Publication (BEIESP)